J Neurophysiol 96: 2857–2867, 2006.
First published August 30, 2006; doi:10.1152/jn.00582.2006.

Hybrid Systems Analysis of the Control of Burst Duration by Low-Voltage-Activated Calcium Current in Leech Heart Interneurons

Andrey Olypher,[1] Gennady Cymbalyuk,[2] and Ronald L. Calabrese[1]
[1]*Department of Biology, Emory University; and* [2]*Department of Physics and Astronomy, Georgia State University, Atlanta, Georgia*

Submitted 3 June 2006; accepted in final form 26 August 2006

Olypher, Andrey, Gennady Cymbalyuk, and Ronald L. Calabrese. Hybrid systems analysis of the control of burst duration by low-voltage-activated calcium current in leech heart interneurons. *J Neurophysiol* 96: 2857–2867, 2006. First published August 30, 2006; doi:10.1152/jn.00582.2006. The leech heartbeat CPG is paced by the alternating bursting of pairs of mutually inhibitory heart interneurons that form elemental half-center oscillators. We explore the control of burst duration in heart interneurons using a hybrid system, where a living, pharmacologically isolated, heart interneuron is connected with artificial synapses to a model heart interneuron running in real-time, by focusing on a low-voltage-activated (LVA) calcium current I_{CaS}. The transition from silence to bursting in this half-center oscillator occurs when the spike frequency of the bursting interneuron declines to a critical level, f_{Final}, at which the inhibited interneuron escapes owing to a build-up of the hyperpolarization-activated cation current, I_h. We varied I_{CaS} inactivation time constant either in the living heart interneuron or in the model heart interneuron. In both cases, varying I_{CaS} inactivation time constant did not affect f_{Final} of either interneuron, but in the varied interneuron, the time constant of decline of spike frequency during bursts to f_{Final} and thus the burst duration varied directly and nearly linearly with I_{CaS} inactivation time constant. Bursts of the opposite, nonvaried interneuron did not change. We show also that control of burst duration by I_{CaS} inactivation does not require synaptic interaction by reconstituting autonomous bursting in synaptically isolated living interneurons with injected I_{CaS}. Therefore inactivation of LVA calcium current is critically important for setting burst duration and thus period in a heart interneuron half-center oscillator and is potentially a general intrinsic mechanism for regulating burst duration in neurons.

INTRODUCTION

Rhythmic bursting activity is a characteristic feature of central pattern generators (CPGs) that drive rhythmic behaviors (Kiehn et al. 2000; Marder and Calabrese 1996) and is involved in the transmission of sensory information (Derjean et al. 2003; Krahe and Gabbiani 2004), in the formation and retrieval of memories (Lisman 1997; Pike et al. 1999), and in other fundamental functions of nervous systems. In CPGs and other bursting networks, the burst period, consisting of the burst duration and the interburst interval, can be modified according to functional demands, such as locomotor speed, by altering the interburst interval (see e.g., Sorensen et al. 2004) and/or the burst duration. The duration of the excited state (e.g., plateau potential that drives spiking activity) determines in large part the burst duration (Crunelli et al. 2005; Marder 1991). The excited state is often sustained by slow inward currents the inactivation/decay of which thus ultimately determines burst duration (Crunelli et al. 2005; Harris-Warrick 2002; Sohal et al. 2006).

The timing network of the leech heartbeat CPG has been subject to intense study of endogenous and network mechanisms contributing to bursting in situ (Calabrese 1995). Here a pair of mutually inhibitory neurons forms the smallest functional network, an elemental oscillator (Hill et al. 2001), that produces continuous alternating bursting activity. The component interneurons of these elemental oscillators permit the application of the full power of the hybrid system approach, already exploited successfully in a number of studies (Le Masson et al. 2002; Manor and Nadim 2001; Sorensen et al. 2004; Szucs et al. 2000), by connecting one living heart interneuron, pharmacologically isolated from its opposite interneuron, with artificial synapses to a model heart interneuron running in real time (Sorensen et al. 2004).

Modeling studies indicate that the burst duration of a leech heart interneuron in a half-center oscillator (Fig. 1*A*) is regulated by the interneuron itself (intrinsically) and by the opposite interneuron (Hill et al. 2001; Sorensen et al. 2004). Soon after the beginning of a burst spike frequency reaches its maximal value and then declines monotonically to a final value of spike frequency at the end of the burst, f_{Final}. This f_{Final} represents the final effective level of inhibition from which the opposite interneuron is able to escape and thus f_{Final} appears to be critical for the transition between bursting and inhibited states. The escape is effected by the activation of the hyperpolarization-activated current I_h. Sorensen et al. (2004), using a hybrid systems approach, demonstrated that the interburst interval of the inhibited interneuron is regulated by its maximal conductance ($\bar{g}_h$) of I_h. A greater $\bar{g}_h$ allows the inhibited interneuron to escape a greater level of inhibition corresponding to a higher value of f_{Final} and thus shorter burst duration of the bursting interneuron. In other words, I_h intrinsically regulates interburst interval of the escaping interneuron, but it also indirectly determines the burst duration of the opposite interneuron.

Here we explore the intrinsic mechanisms by which burst duration in heart interneurons is controlled using a hybrid system approach that focused on low-voltage-activated (LVA) calcium current. In heart interneurons, LVA calcium current consists of two components: I_{CaF}, which activates and inactivates quickly, and I_{CaS}, which activates and inactivates slowly (Ivanov and Calabrese 2000, 2003; Lu et al. 1997; Olsen and Calabrese 1996). Modeling studies indicate that I_{CaF} contributes mainly to the burst initiation, whereas I_{CaS} determines

Address for reprint requests and other correspondence: R. L. Calabrese, Dept. of Biology, Emory University, 1510 Clifton Rd. N.E., Atlanta, GA 30322 (E-mail: rcalabre@biology.emory.edu).

The costs of publication of this article were defrayed in part by the payment of page charges. The article must therefore be hereby marked "*advertisement*" in accordance with 18 U.S.C. Section 1734 solely to indicate this fact.

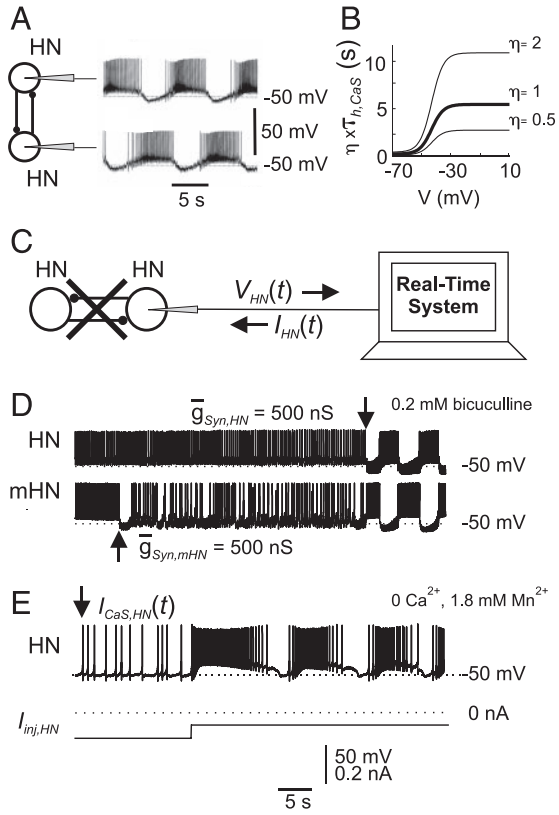

FIG. 1. Experimental paradigm. *A*: intracellular recordings showing characteristic alternating bursting of mutually inhibitory leech heart (HN) interneurons (half-center oscillator) in an isolated ganglion. *B*: time constant of I_{CaS} inactivation, $\tau_{h,Cas}$, as used in the canonical model (thick line) and when scaled (i.e., multiplied) by the factor η equal to 0.5 and 2 (thin lines). *C*: dynamically clamped, pharmacologically isolated heart interneuron receiving either synaptic current I_{SynS} or I_{CaS} or both calculated in the real-time system (see METHODS). The mathematical model of the heart interneuron, in the case of the hybrid half-center oscillator, also ran in the real-time system. *D*: typical behavior of a living heart (HN) interneuron and a model heart (mHN) interneuron after adding inhibitory synaptic currents to them (arrows). Bursting did not start when only 1 neuron, mHN interneuron here, was inhibited by the other (left arrow). After the inhibition became reciprocal (right arrow), alternating bursting started almost immediately. The traces are from an experiment in which synaptic interaction between the living heart interneurons in the ganglion preparation was blocked with 0.2 mM bicuculline methiodide. *E*: typical initiation of bursting in a living heart interneuron with its I_{SynS} and I_{CaS} blocked in Ca^{2+}-free Mn^{2+} saline. Injecting of the artificial calcium current $I_{CaS,HN}$ alone (arrow), even with a large maximal conductance, was often not sufficient to initiate bursting. In these cases, constant hyperpolarizing current ($I_{inj,HN}$) was added. In this example, bursting started after a step-wise increase of $I_{inj,HN}$ to from -0.2 to -0.1 nA; $\bar{g}_{CaS,HN} = 20$ nS.

burst duration (Hill et al. 2001). Hill et al. (2001) explored the consequences of the bilateral variation of I_{CaS} inactivation time constant in the model elemental oscillator. Their simulations led to the hypothesis that the I_{CaS} inactivation time constant controls burst duration by determining the spike frequency decay during the burst to f_{Final}, with slow inactivation corresponding to long bursts and fast inactivation corresponding to short bursts. Here we varied I_{CaS} inactivation time constant either in the living heart interneuron or in the mathematical model (Hill et al. 2001) of the heart interneuron in a hybrid elemental oscillator in which artificial synapses and I_{CaS} were implemented in the living neuron using dynamic clamp (Goaillard and Marder 2006; Prinz et al. 2004; Robinson and Kawai 1993; Sharp et al. 1993). Our results support this hypothesis and suggest that inactivation of LVA calcium current sets burst duration and thus period in a heart interneuron half-center oscillator and is potentially a general intrinsic mechanism for regulating burst duration in neurons.

METHODS

Leeches (*Hirudo medicinalis*) were obtained from Leeches USA (Westbury, NY) and maintained in artificial pond water at 15°C. After the animals were anesthetized in ice-cold saline, individual ganglia were dissected and pinned ventral-side-up in Petri dishes lined with silicone elastomer (Sylgard, Dow Corning, Midland, MI; bath volume: 0.5 ml). The methods for preparing and maintaining leech ganglia and for identifying heart interneurons for electrophysiological recording have been previously described (Lu et al. 1997).

The ganglionic sheath over the cell bodies was removed with fine microscissors or scalpels. Ganglia were superfused continuously with normal leech saline containing (in mM) 115 NaCl, 4 KCl, 1.8 $CaCl_2$, 10 glucose, and 10 HEPES buffer, adjusted to pH 7.4. All experiments were performed on heart interneurons in an isolated midbody segmental ganglion 3 or 4. Heart interneurons were identified based on soma size, soma location in the ganglion, and ultimately by their characteristic bursting activity (Fig. 1*A*). Heart interneurons were isolated pharmacologically with 0.2 mM bicuculline methiodide (Sigma, St. Louis, MO) added to normal saline. In some experiments, all Ca^{2+} in normal saline was replaced with 1.8 mM Mn^{2+} to block calcium currents and synaptic interaction between heart interneurons (Ca^{2+}-free Mn^{2+} saline). The robustness of bursting of heart interneuron in of Ca^{2+}-free Mn^{2+} saline was assessed quantitatively (see following text).

Microelectrodes for both intra- and extracellular recordings were made from borosilicate glass tubes (A-M Systems) 1 mm OD, 0.75 mm ID. Sharp microelectrodes for intracellular recordings were filled with 4 M potassium acetate with 20 mM KCl (20–35 MΩ). Currents were injected using discontinuous single-electrode current clamp (Axoclamp 2A, Axon Instruments, Foster City, CA). Sample rates were between 2.5 and 3 kHz. The electrode potential was monitored on an oscilloscope to ensure that it had settled between current injection cycles. At the end of the experiment, microelectrodes were withdrawn from the cell, and only if the bath potential measured by the electrode was within the range ±5 mV were the data accepted. As in Sorensen et al. (2004), high input resistance was critical for the successful establishment of rhythmic bursting in hybrid half-center oscillators. Lower input resistances due to poor penetration and consequent decreased membrane time constant reduced the cell's ability to integrate inhibitory synaptic currents injected with dynamic clamp. Only neurons with input resistance >60 MΩ were accepted.

Extracellular recordings were obtained as described in (Masino and Calabrese 2002) with suction electrodes pulled to 20–30 μm tip diameters and filled with normal saline. Weak suction was applied with a syringe, and the cell body was drawn into the electrode so that it fit snugly. Extracellular signals were amplified with a differential AC amplifier (A-M Systems model 1700). All experimental data were digitized and stored using pCLAMP software (Axon Instruments, Union City, CA).

To produce hybrid half-center oscillators, we used dynamic clamp (Goaillard and Marder 2006; Prinz et al. 2004; Robinson and Kawai 1993; Sharp et al. 1993) to establish reciprocal artificial inhibitory synapses between a living heart interneuron (synaptically isolated with 0.2 mM bicuculline methiodide or Ca^{2+}-free Mn^{2+} saline) and a model of an oscillator heart interneuron running in real time. We also used dynamic clamp to introduce a conductance corresponding to the low-threshold slowly inactivating calcium current I_{CaS} (Angstadt and Calabrese 1991) into the living heart interneurons when endogenous calcium currents were blocked by Ca^{2+}-free Mn^{2+} saline. In the same saline, we also studied the control of bursting by I_{CaS} in the

isolated living interneuron. In these hybrid system experiments, we used the single-compartment model of the heart interneuron described by Hill et al. (2001) with the following changes in the parameters of the model: the leak current was altered by setting the maximal conductance $\bar{g}_L = 9$ nS and the reversal potential $E_L = -62$ mV instead of $\bar{g}_L = 8$ nS, $E_L = -60$ mV and graded synaptic transmission was not included, $\bar{g}_{SynG} = 0$ nS.

Dynamic clamp I_{CaS} was calculated according to the following equations (Hill et al. 2001)

$$I_{CaS} = \bar{g}_{CaS} m_{CaS}^2 h_{CaS} (V - E_{CaS})$$

$$\frac{dm_{CaS}}{dt} = \frac{m_{\infty,CaS}(V) - m_{CaS}}{\tau_{m,CaS}(V)}$$

$$\frac{dh_{CaS}}{dt} = \frac{h_{\infty,CaS}(V) - h_{CaS}}{\eta \tau_{h,CaS}(V)} \quad (1)$$

where V was the membrane potential (in V), t was time (in s), $E_{CaS} = 0.135$ V, $\bar{g}_{CaS} = 3.2$ nS, and

$$m_{\infty,CaS}(V) = 1/(1 + e^{-420(V+0.047)})$$

$$\tau_{m,CaS}(V) = 0.005 + 0.134/(1 + e^{-400(V+0.049)})$$

$$h_{\infty,CaS}(V) = 1/(1 + e^{360(V+0.055)})$$

$$\tau_{h,CaS}(V) = 0.2 + 5.25/(1 + e^{-250(V+0.043)}) \quad (2)$$

with $\tau_{m,CaS}$ and $\tau_{h,CaS}$ in s.

In *Eq. 1*, η was used as a scaling factor for the time constant $\tau_{h,CaS}$ of the inactivation variable. In the canonical model of Hill et al. (2001) it is set equal to 1; here it was varied from 0.25 to 4 with $\eta = 1$ being the canonical or benchmark value against which variations were considered.

Dynamic-clamp synapses were implemented according to the following equations (Cymbalyuk et al. 2002a,b)

$$I_{SynS} = \bar{g}_{SynS} Y_{post} M_{post} (V_{post} - E_{Syn}), \quad \frac{dY_{post}}{dt} = \frac{X_{post} - Y_{post}}{\tau_2}$$

$$\frac{dX_{post}}{dt} = \frac{X_\infty(V_{pre}) - X_{post}}{\tau_1}, \quad \frac{dM_{post}}{dt} = \frac{M_\infty(V_{pre}) - M_{post}}{0.2}$$

$$M_\infty(V_{pre}) = 0.1 + \frac{0.9}{1 + e^{-1000(V_{pre}+0.04)}} \quad (3)$$

where the rise time constant $\tau_1 = 2$ ms and decay constant time $\tau_2 = 11$ ms, the maximal conductance of the spike-mediated synaptic transmission $\bar{g}_{SynS}$ was in the range of 300–600 nS, reversal potential $E_{Syn} = -62$ mV. The function $X_\infty(V_{pre})$ was equal to 1 for 5 ms after V_{pre} exceeded -10 mV; otherwise it was equal to zero. Both dynamic-clamp calculations and the model of the heart interneuron were implemented in Simulink (MathWorks, Natick, MA) and ran on a dedicated real-time signal processing controller board (DS1103; dSPACE, Paderborn, Germany). In analysis involving a model half-center oscillator

$$X_\infty(V_{pre}) = \frac{1}{1 + e^{-1000(V_{pre}+0.01)}} \quad (4)$$

exactly as in (Cymbalyuk et al. 2002a,b; Sorensen et al. 2004). The difference between the step-wise function $X_\infty(V_{pre})$ in *Eq. 3* and the smooth sigmoid function in *Eq. 4* is negligible. The step-wise form was chosen for hybrid system experiments because it was much easier to implement it in the real-time system. In the model half-center oscillator, $\bar{g}_{SynS}$ was set to 150 nS to obtain a period similar to the average period observed in the experiments with hybrid half-center oscillators.

The model leech heart interneuron (Hill et al. 2001) is described by the system of 14 ordinary differential equations. The spike-mediated synaptic current is described by three differential equations (see *Eq. 3*). Thus implementation of a hybrid half-center oscillator meant solving a system of 20 ordinary differential equations in real time. Two extra differential equations were required for calculating I_{CaS} (see *Eq. 1*). The differential equations were integrated using the direct Euler method with a time step of 0.1 ms. The accuracy was confirmed by solving the same equations with the highly accurate variable-order Matlab solver *ode15s*.

We have written a Simulink library of functions and blocks for implementing all membrane and synaptic currents described for the leech heart interneuron. Using this library, we ported the mathematical model of the heart interneuron into Simulink and compiled it with RTI (Real-Time Interface; dSPACE, Paderborn, Germany), as a stand-alone real-time application for a DS1103 PPC Controller Board. As a part of the hybrid system, the model ran in real-time at a rate of 20 kHz. ControlDesk (dSPACE, Paderborn, Germany) interface allowed the loading of the hybrid model into the board and changing parameters of the model on the fly during the experiment. The library can be used for implementing voltage-dependent currents that have been described in other neurons. For a similar approach see e.g., Debay et al. (2004).

In forming a hybrid half-center oscillator, synaptic conductances were always implemented as follows (Fig. 1*D*). First, the maximal synaptic conductance in the model heart interneuron, $\bar{g}_{SynS,mHN}$, was set to a starting value of 300 nS. If the model heart interneuron continued tonic firing at a high rate, $\bar{g}_{SynS,mHN}$ was increased, the aim being to get the model heart interneuron to fire tonically at a low rate or even sporadically. Then, $\bar{g}_{SynS,mHN}$ in the living heart interneuron was set to 500 nS. After that, the spiking of the model heart interneuron most often inhibited the living heart interneuron and the alternating bursting started. Sometimes, it was useful to increase $\bar{g}_{SynS,mHN}$ to 600 nS to obtain effective inhibition of the living heart interneuron. In some cases, when the model heart interneuron fired too weakly, it was necessary to suppress transient firing in living heart interneuron by injecting a small hyperpolarizing current (-0.1 nA).

Analyses of burst characteristics were performed off-line with scripts written in Matlab (MathWorks). As in Sorensen et al. (2004), the times of occurrence of action potentials (spikes) were found by first detecting time intervals when the membrane potential was above a specific threshold. For intracellular recordings, the threshold was chosen to be -20 mV, for extracellular recordings the threshold was variable. If the interval was <0.5 ms, it was discarded as a likely consequence of the digitization error or noise. All other time intervals were associated with spikes. The time of occurrence of a spike was taken as the moment of time within the interval when the membrane potential reached its maximum. Spikes that occurred within <2 ms from preceding spikes were considered as spurious and excluded. Bursts were defined as sequences of at least five spikes such that intervals between the spikes were <0.5 s. This rule allowed us to exclude sporadic spikes at the beginning and end of bursts. At least seven consecutive bursts per experimental trial were used for the analyses.

To characterize and analyze the burst pattern, we calculated burst durations, periods of half-center oscillations, and final frequencies of the bursts. The burst duration was calculated as the time between the first spike of a burst and the last spike of that burst. The period was calculated as the time between the median spike of one burst and the median spike of the next burst. Spike frequencies were defined as the inverse of the corresponding ISI. In particular, the final spike frequency (f_{Final}) was defined as the inverse to the last ISI in the burst.

In experiments in Ca^{2+}-free Mn^{2+} saline, where heart interneurons were injected only with I_{CaS} but not with I_{SynS}, burst plateaus had no spikes at their ends. Therefore in these experiments, the end of the burst was estimated on the basis of the averaged membrane potential V_{avg}. V_{avg} was calculated as a moving average. The window for the averaging did not exceed 400 ms; variations of the window in the range of hundred milliseconds had minor influence on results. The end

of a burst was defined as the moment of time when V_{avg} attained 98% of its minimum value in the interval between the first spike of the burst and the first spike of the next burst. Use of the 98% minimum V_{avg} eliminated the effect of noise in ascertaining the minimum, and small variations of percentage minimum V_{avg} had negligible effect on the results. Period was then calculated as the differences between two consecutive ends of bursts.

Variability in the period was used as a measure of the regularity of bursting and correspondingly as a measure of data quality. A preparation was considered to show regular bursting, if not more than one trial had a coefficient of variation of the period, cv_T, >20% with all the other trials having $cv_T < 20\%$. Only the data from trials with $cv_T < 20\%$ from regular preparations were accepted for the further analyses.

To assess the time constant of spike frequency decline during a burst, we considered all spike frequencies in the burst starting from the maximal one and used the least-square exponential fit with a function of the form $Ae^{-t/\tau}$ (Fig. 2*A*). The fit was made for every burst in a trial. Only the fits, accounting for at least 50% of the total variance were considered as acceptable. A trial had to have at least five bursts with accepted fits to be analyzed further. For each trial, all the accepted time constants τ's were averaged. To assess the time constant of I_{CaS} inactivation during a burst, we used double-exponential fits of g_{CaS} with functions of the form $Ae^{-t/\tau_1} + Be^{-t/\tau_2}$ (Willms et al. 1999) and applied the same fit criteria (Fig. 2*B*). We did not apply the double-exponential fit for spike frequencies because in many cases there were not many spikes in the initial phase of the burst before the pair of spikes that had the smallest interspike interval. Fits were made with Matlab (MathWorks) *fit* function using Levenberg-Marquardt method. To assess the effective value of $\tau_{h,CaS}$ during a burst, $\tau_{h,CaS}$ was first averaged within spikes. Such averaging removed fast changes of $\tau_{h,CaS}$ caused by fast changes of the membrane potential. Then these spike averaged values were averaged across all the spikes in the burst.

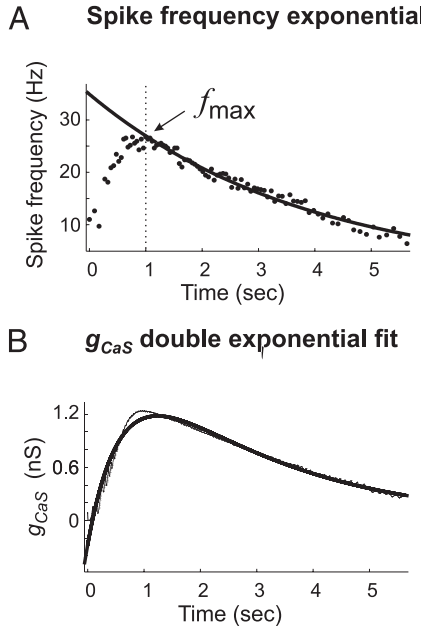

FIG. 2. Assessment of the time constants of decay of spike frequency and I_{CaS} conductance during a burst. *A*: example of an exponential fit of spike frequency decline during a burst of a living heart interneuron with artificial I_{CaS} having the canonical inactivation time constant ($\eta = 1$). The fit was performed for frequencies succeeding the maximal one. Fit equation: $34.9\exp^{-}t[r]^{/3.97}$, $r^2 = 0.98$, RMSE = 0.88. *B*: double-exponential fit of g_{CaS} for the same burst as in *A*. Fit equation: $2.48\exp^{-}t[r]^{/3.97}$, $r^2 = 0.98$, RMSE = 0.05; the decay time constant was always the greater of the 2 in the equation, in this example 2.68 s. The data are from a living heart interneuron (Ca^{2+}-free Mn^{2+} saline) in a hybrid half-center oscillator with artificial I_{CaS} having the canonical inactivation time constant ($\eta = 1$).

Values reported here are the means ± SD across experiments except as indicated. Statistical analyses included one-way ANOVAs, multiple comparisons of means with the Bonferroni *t*-test, and correlation analyses. The analyses were performed in Matlab (ANOVA, Bonferroni *t*-test) and KaleidaGraph (Synergy Software, Reading, PA) (correlation analyses). A cutoff of $P = 0.05$ was used to determine statistical significance. To simplify the presentation of the multiple comparisons, comparisons to a single chosen value of the varied parameter $\eta = 1$ are indicated on figures.

RESULTS

Here we wished to explore the intrinsic cellular mechanism that determines burst duration in heart interneurons. Previous modeling studies (Hill et al. 2001) showed that burst duration is directly regulated by the time constant of inactivation of I_{CaS} during a burst because this inactivation determines how quickly the spike frequency declines to the critical final value, f_{Final}, at which escape, intrinsically set by $\bar{g}_h$, of the opposite interneuron is possible. At depolarized potentials, as during a burst, the time constant of the inactivation variable of I_{CaS}, $\tau_{h,CaS}$, reflects inactivation of I_{CaS}, and it is the longest time constant in the model system. Thus during a burst I_{CaS} operates relatively independently from other intrinsic currents. Hill et al. (2001) varied the inactivation time constant symmetrically in both interneurons of a model half-center oscillator (Fig. 1*A*). Here we varied I_{CaS} inactivation kinetics in only one interneuron of the pair both in model half-center oscillators and in hybrid half-center oscillators composed of a model and a living neuron and assessed the effects on the burst characteristics (burst duration, period, f_{Final}) of both the varied and unvaried neuron. By making these changes unilaterally (i.e., asymmetrically), we could focus on pinpointing the effects of the change intrinsic to the varied neuron, much as was done by Sorensen et al. (2004) to isolate the intrinsic effects of changes in $\bar{g}_h$. We also explored the effects of I_{CaS} inactivation kinetics on endogenous bursting in a pharmacologically isolated heart interneuron. To change the kinetics, we scaled the canonical time constant $\tau_{h,CaS}$ of the inactivation variable h_{CaS} (see *Eq. 1*) by a constant scaling factor η (Fig. 1*B*). Although this method of linear scaling affects both inactivation and de-inactivation kinetics, the effects on de-inactivation are small (in the voltage range where de-inactivation occurs $\tau_{h,CaS}$ is small compared with the interburst interval and the linear scaling does not alter it significantly with respect to this interval) (Fig. 1*B*). Thus as demonstrated directly in the following text, our method is suitable for changing the observable time constant of inactivation of I_{CaS} during a burst and subsequently we will refer to changing the time constant of I_{CaS} inactivation.

To assess the effects of changes of I_{CaS} inactivation time constant in living interneurons, we used dynamic clamp (Goaillard and Marder 2006; Prinz et al. 2004; Robinson and Kawai 1993; Sharp et al. 1993). Dynamic clamp allowed us to implement I_{CaS} with the desired inactivation kinetics in the intracellularly recorded heart interneuron. Hybrid half-center oscillators, consisting of a living heart interneuron and the mathematical model of an oscillator heart interneuron (Hill et al. 2001) were created by using dynamic clamp to implement not only I_{CaS} but also synaptic currents between the model

TABLE 1. *Specification of the experiments*

Varied	Unvaried	$I_{CaS,HN}$	Artificial Synapses in HN and mHN	Saline
mHN	HN	No	Yes	0.2 mM bicuculline
HN	mHN	Yes	Yes	0 Ca^{2+}, 1.8 mM Mn^{2+}
HN	—	Yes	No	0 Ca^{2+}, 1.8 mM Mn^{2+}

Varied, the heart interneuron, living (HN) or model (mHN), in which I_{CaS} inactivation time constant was varied. Unvaried, the interneuron with the unvaried I_{CaS} inactivation time constant. $I_{CaS,HN}$, artificial low-voltage-activated A calcium current injected or not into the HN interneuron.

interneuron and the living heart interneuron (Cymbalyuk et al. 2002b; Sorensen et al. 2004) (Fig. 1, *C–E*, Table 1).

Model half-center oscillator: unilateral variation of I_{CaS} inactivation time constant

First we analyzed the effects of varying the I_{CaS} inactivation time constant in one neuron (varied) of a model half-center oscillator while the other neuron (constant) remained at the canonical value to establish benchmark measurements and so we could compare results in hybrid half-center oscillators directly to our model. The results of our simulations are illustrated in Figs. 3 and 4*A*. When I_{CaS} inactivation time constant was at canonical levels in the varied model neuron ($\eta = 1$) normal symmetric alternating bursting was observed. During each burst g_{CaS} decayed smoothly and the inactivation variable h_{CaS} declined in step albeit more slowly (not shown). We measured the time constant of g_{CaS} decay during the burst in the varied model neuron as an estimate of the time constant of I_{CaS} inactivation during a representative burst (not shown but as illustrated in Fig. 2*B*) and obtained a value of ~3.6 s and also measured the time constant of decay of h_{CaS} during the burst and obtained a value of ~4.0 s. We directly assessed the effective value of $\tau_{h,CaS}$ during the burst (according to *Eq. 2* with smoothing; see METHODS), and we obtained an average value of ~4.0 s near our estimate from the decay of h_{CaS}. Analysis of I_{CaS} state variables showed that the discrepancy between the time constant of h_{CaS} decay and g_{CaS} decay arises because of some deactivation of I_{CaS} associated with slow voltage decline during the burst. We chose the time constant of g_{CaS} decay as a benchmark metric not only because it corresponds to the most experimentally accessible measure of I_{CaS} inactivation but primarily because as will be shown below the decay of g_{CaS} directly controls burst duration through its effect on spike frequency. We also measured the time constant of spike frequency decay during the burst in the varied neuron as a benchmark (not shown but as illustrated in Fig. 2*A*) to be compared with the time constant of g_{CaS} decay and obtained a value of ~6.7 s. We then applied these two benchmark measures, g_{CaS} decay time constant and spike frequency decay time constant, to our subsequent analyses of the effect of varying I_{CaS} inactivation time constant (η) in model and hybrid half-center oscillators.

Decreasing I_{CaS} inactivation time constant (η) in one "neuron" of a model half-center oscillator decreased the burst duration in the varied neuron and the period of the oscillations (Fig. 3*B*, $\eta = 0.5$), while increasing I_{CaS} inactivation time constant had the opposite effects (Fig. 3*B*, $\eta = 4$). These manipulations had little effect on the final frequency of either the varied or the constant model neuron. Over the range tested ($\eta = 0.5, 1, 2, 4$) increasing I_{CaS} inactivation time constant led to a steady increase in the burst duration of the varied model neuron (>300%) with little variation in the burst duration of the constant model neuron (~25% reduction; Fig. 3*B*). The period of the oscillations also increased (Fig. 3*B*), albeit less (~150%), reflecting a change in step with the burst duration of the varied model neuron and no increase in the burst duration of the constant model neuron. The final frequency of the two neurons varied somewhat but nonmonotonically and over a very limited range (<21%; Fig. 3*B*). The time constant of g_{CaS} decay in the varied model neuron scaled linearly with η, whereas that of the constant model neuron remained relatively unchanged (Fig. 4*A*, *left*). Moreover, in the varied neuron the time constant of decay of spike frequency was strongly correlated with the time constant of decay of g_{CaS} (Fig. 4*A*, *right;*

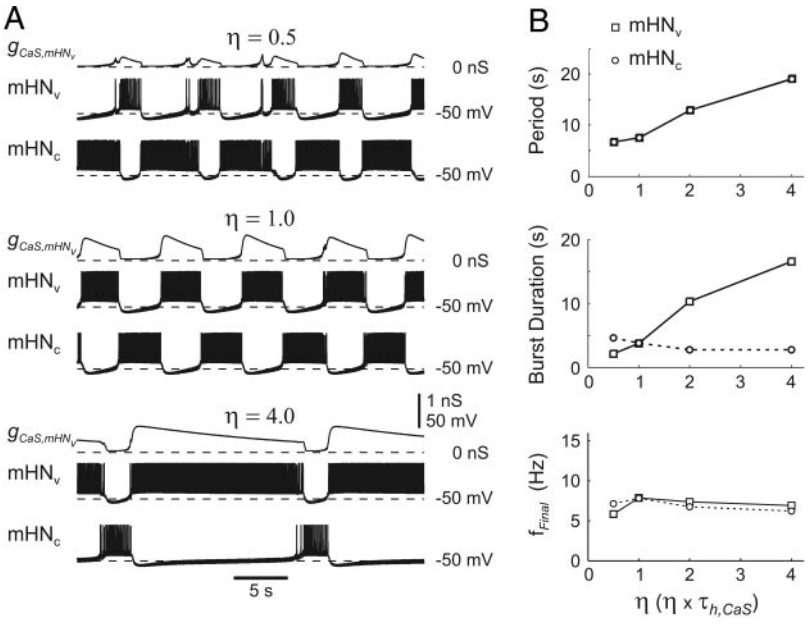

FIG. 3. Model half-center oscillator: control of the burst duration of a model interneuron by its own I_{CaS} inactivation time constant. *A*: typical behavior of a model half-center oscillator for 3 different scaling factors of I_{CaS} inactivation time constant: $\eta = 0.5$ (*top,* faster inactivation), $\eta = 1$ (*middle,* inactivation as in the canonical model), and $\eta = 4$ (*bottom,* slower inactivation). The membrane potentials of the varied (mHN_v) and the canonical (unvaried) (mHN_c) model heart interneurons and the calcium conductance ($g_{CaS,\ mHNv}$) of the varied model interneuron are shown. When I_{CaS} inactivation time constant was half that of the canonical model ($\eta = 0.5$), the mHN_v interneuron showed burst fragmentation (*top*). Burst duration increased in the mHN_v interneuron with increasing η but was relatively constant in the mHN_c interneuron. *B*: increasing I_{CaS} inactivation time constant (increasing η) caused an increase in the period of the half-center oscillator (*top*), an increase of mHN_v interneuron's burst duration (*middle*) with a small decrease of mHN_c interneuron's burst duration, and little change in the final spike frequencies (f_{Final}) of either model interneuron (*bottom*).

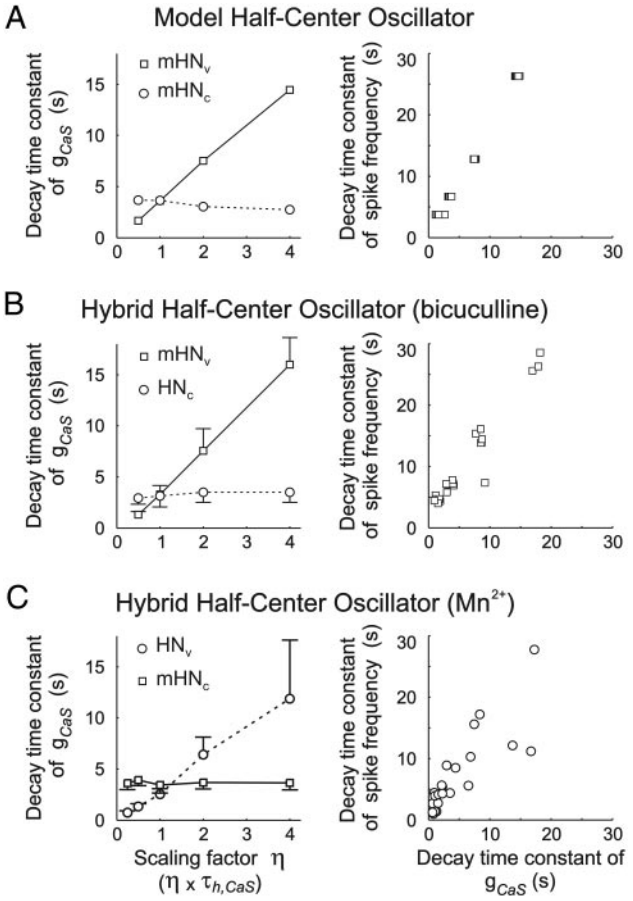

FIG. 4. Correlated decay of $\bar{g}_{CaS}$ and spike frequency during a burst in model and hybrid half-center oscillators. *A*: model half-center. Increase of the I_{CaS} inactivation time constant in the varied model heart (mHN$_v$) interneuron led to a near linear increase of the decay time constant of g_{CaS}[r] in the mHN$_v$ interneuron but not in the unvaried model (mHN$_c$) interneuron (*left*). Linear correlation between the decay time constants of spike frequency and g_{CaS} in the mHN$_v$ interneuron (*right*). *B*: hybrid half-center. Increase of the I_{CaS} inactivation time constant in the model heart (mHN$_v$) interneuron led to a near linear increase of the decay time constant of g_{CaS} in the mHN$_v$ interneuron but not in the unvaried living (HN$_c$) interneuron (*left*). Linear correlation between the decay time constants of spike frequency and g_{CaS} in the mHN$_v$ interneuron (*right*). *C*: hybrid half-center. Increase of the I_{CaS} inactivation time constant in the living heart (HN$_v$) interneuron led to a near linear increase of the decay time constant of g_{CaS} in the HN$_v$ interneuron but not in the unvaried model (mHN$_c$) interneuron (*left*). Linear correlation between the decay time constants of spike frequency and g_{CaS} in the HN$_v$ interneuron (*right*).

$r^2 = 0.99$; $n = 61$, $P = 3.7 \times 10^{-70}$), albeit slower. For the constant model neuron there was no significant correlation between these time constants (not shown; $r^2 = 0.21$; $n = 63$, $P = 0.09$). These results indicate that the scaling factor (η) used to scale linearly $\tau_{h,CaS}$, scales the time constant of g_{CaS} decay. Burst duration is indeed controlled by inactivation of I_{CaS}, and this inactivation is associated with a parallel decline in spike frequency. The final frequency does not vary with I_{CaS} inactivation time constant, indicating that the escape point of the opposite cell in the half-center oscillator is not affected.

For greater reductions in I_{CaS} inactivation time constant ($\eta = 0.25$), the burst fragmentation already noticeable in the records for $\eta = 0.5$ renders the bursting so irregular that the burst criterion was not met (see METHODS), and the data were not considered for analysis. Hill et al. (2001) varied I_{CaS} inactivation time constant bilaterally in the model half-center oscillator and observed regular bursting even for comparable reductions in I_{CaS} inactivation time constant. To test the hypothesis that the irregularity we observed was caused by the broken symmetry in the model, we performed simulations of the model with both neurons having greatly reduced I_{CaS} inactivation time constant ($\eta = 0.25$). The resulting bursting was very regular, supporting this hypothesis.

Hybrid half-center oscillator

UNILATERAL VARIATION OF I_{CAS} INACTIVATION TIME CONSTANT IN THE MODEL HEART INTERNEURON. We next used hybrid half-center oscillators composed of a living heart interneuron and a model heart interneuron to explore the effect of I_{CaS} inactivation time constant on burst duration. We first varied $\tau_{h,CaS}$ unilaterally in the model heart interneuron (mHN$_v$) (Fig. 5, Table 1). The living heart interneuron (HN$_c$) was synaptically isolated with bicuculline (0.2 mM). When reciprocally connected with artificial inhibitory synapses to form a hybrid half-center oscillator, the living heart interneuron and the model heart interneuron produced regular alternating bursting (Fig. 1*A*). In the example illustrated in Fig. 5*A*, $\eta = 1$, the period was 6.0 ± 0.8 s and burst durations were 2.8 ± 0.6 and 3.1 ± 0.8 s for the model and living interneurons, respectively. We then varied the inactivation time constant of I_{CaS} in the model neuron using the scaling factor η as described in the previous section ($\eta = 0.25$, 0.5, 1, 2, 4 in pseudo-random order). In the case of $\eta = 0.25$, the bursting pattern was regular only in two of seven preparations (regularity, as defined in METHODS, meant that the coefficients of variation of burst periods of both living and model heart interneurons were <20%), and these data were not included in our analyses.

In the example illustrated in Fig. 5*A*, decreasing I_{CaS} inactivation time constant (η) in model neuron of the hybrid half-center oscillator decreased its burst duration and the period of the oscillations (Fig. 5*A*, $\eta = 0.5$), whereas increasing I_{CaS} inactivation time constant had the opposite effects (Fig. 5*A*, $\eta = 4$). These manipulations had little effect on the burst duration of the living neuron or on the final frequency of either the model or living neuron. Figure 5*B* shows averaged data across preparations ($n = 6$). The period and the burst duration of the model neuron increased monotonically with η (Fig. 5*B*, *top* and *middle;* supplementary Table 1[1]), and these effects were statistically significant [ANOVA $F(3,20) = 20.95$; $P = 2.2 \times 10^{-6}$, and $F(3,20) = 13.94$; $P = 3.9 \times 10^{-5}$, respectively]. The f_{Final} increased little with η - by 22% for $\eta = 4$ compared with $\eta = 1$ (Fig. 5*B*, *bottom*), and this effect was not significant [ANOVA $F(3,20) = 1.60$; $P = 0.22$]. As expected, the period was the same for both model and living heart interneurons. The burst duration and f_{Final} of the living neuron remained relatively constant as η was varied and there were no statistically significant effects of this variation [ANOVA $F(3,20) = 3.07$; $P = 5.14 \times 10^{-2}$ and $F(3,20) = 0.28$; $P = 0.84$, respectively].

As found in the simulations of the model half-center oscillator, the decay time constant of g_{CaS} varied linearly with η (Fig. 4*B*, *right*), and there was a strong correlation between the decay time constants of g_{CaS} and of spike frequency in a burst (Fig. 4*B*, *left*; $r^2 = 0.94$; $n = 24$, $P = 1.1 \times 10^{-14}$). Comparison of Fig. 4, *A* and *B*, shows that the variation of I_{CaS} inactivation time constant (η) affects the decay of g_{CaS} and

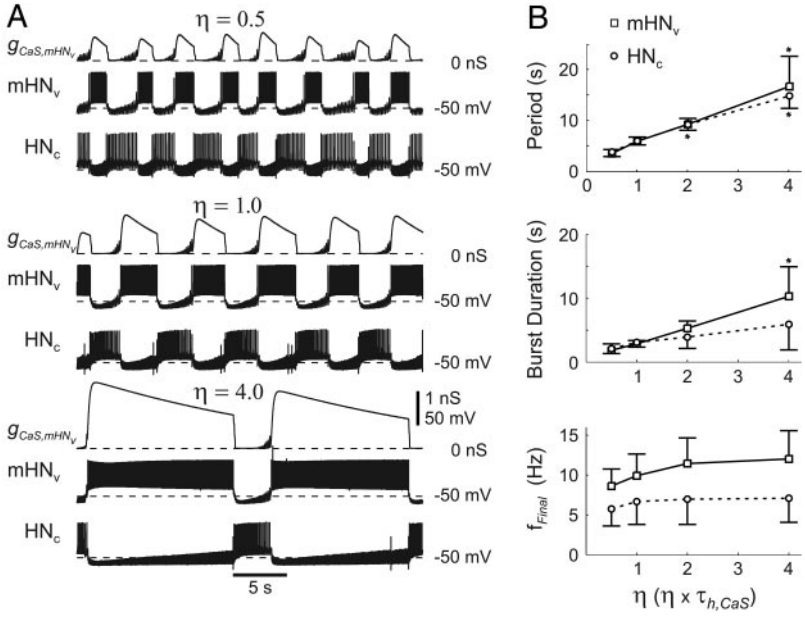

FIG. 5. Hybrid half-center oscillator: control of the burst duration of the model interneuron by its own I_{CaS} inactivation time constant. *A*: typical behavior of a hybrid half-center oscillator for 3 different scaling factors of I_{CaS} inactivation time constant: $\eta = 0.5$ (*top,* faster inactivation), $\eta = 1$ (*middle,* inactivation as in the canonical model), and $\eta = 4$ (*bottom,* slower inactivation). The membrane potentials of the model heart (mHN$_v$) interneuron (varied) and the living heart (HN$_c$) interneuron (unvaried) and calcium conductance ($g_{CaS,\ mHNv}$) of the model heart interneuron are shown. Burst duration increased in the mHN$_v$ interneuron with increasing η but was relatively constant in the HN$_c$ interneuron. *B*: increasing I_{CaS} inactivation time constant (increasing η) in the mHN$_v$ interneuron caused an increase in the period of the half-center oscillator (*top*), an increase of mHN$_v$ interneuron's burst duration (*middle*) but not of the HN$_c$ interneuron's burst duration, and little change in the final spike frequencies (f_{Final}) of either the mHN$_v$ or HN$_c$ interneuron (*bottom*). Asterisks indicate significant differences ($P < 0.05$) between measured values and values corresponding to $\eta = 1$. Normal saline contained 0.2 mM bicuculline methiodide to synaptically isolate the HN$_c$ interneuron.

spike frequency in the model heart interneuron in the same way regardless whether the model interneuron interacts with another model interneuron or a living heart interneuron in a half-center oscillator. For the unvaried living heart interneuron, there was no significant correlation between the decay time constants of g_{CaS} and of spike frequency in a burst ($r^2 = 0.05$; $n = 16$, $P = 0.405$). As in the model, the inactivation of I_{CaS} determined the spike frequency decline in a burst and thus the time necessary to achieve f_{Final} at which the opposite cell can escape from the inhibition.

UNILATERAL VARIATION OF I_{CAS} INACTIVATION TIME CONSTANT IN THE LIVING HEART INTERNEURON. We next used hybrid half-center oscillators to explore the effect of I_{CaS} inactivation time constant on burst duration in the living heart interneuron. We varied $\tau_{h,CaS}$ unilaterally in the living heart interneuron (HN$_v$) using dynamic clamp to inject I_{CaS} with endogenous calcium currents blocked (Ca^{2+}-free Mn^{2+} saline) (Fig. 6, Table 1). In the model heart interneuron (mHN$_c$), $\tau_{h,CaS}$ was not varied ($\eta = 1$). When reciprocally connected with artificial inhibitory synapses to form a hybrid half-center oscillator, the living heart interneuron and the model heart interneuron produced regular alternating bursting. In the example illustrated in Fig. 6*A*, $\eta = 1$, the period was 7.03 ± 1.21 s and burst durations were 3.02 ± 0.43 and 4.14 ± 0.43 s for the model and living interneurons, respectively. We then varied the inactivation time constant of I_{CaS} in the living neuron using the scaling factor η as described in the previous section ($\eta = 0.25, 0.5, 1, 2, 4$ in pseudo-random order). In these experiments, bursting was more stable than in the previous experiments, where the living neuron was synaptically isolated with bicuculline and $\tau_{h,CaS}$ was varied in the model heart interneuron. In particular, the data for $\eta = 0.25$ met our criterion for regularity (see METHODS) in all six preparations.

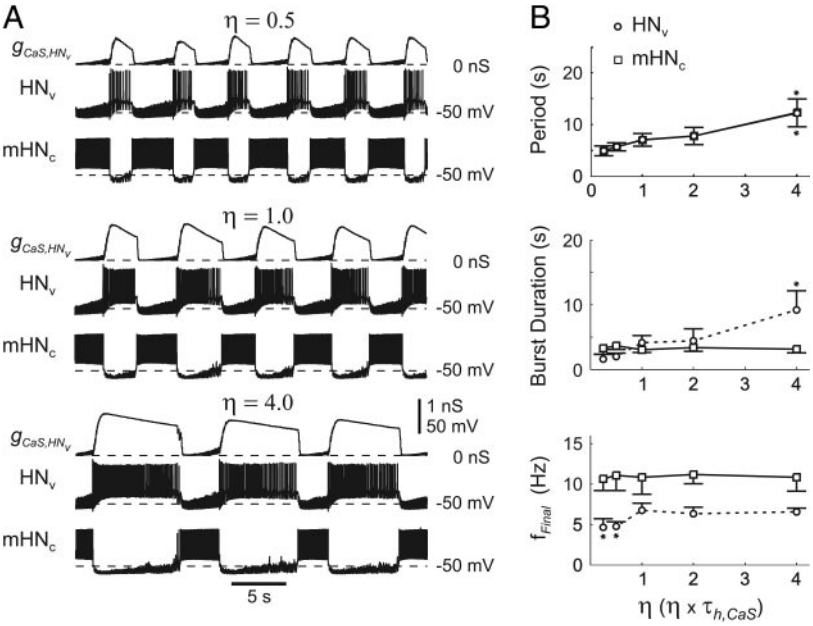

FIG. 6. Hybrid half-center oscillator: control of the burst duration of the living interneuron by its own I_{CaS} inactivation time constant. *A*: typical behavior of a hybrid half-center oscillator for 3 different scaling factors of I_{CaS} inactivation time constant: $\eta = 0.5$ (*top,* faster inactivation), $\eta = 1$ (*middle,* inactivation as in the canonical model), and $\eta = 4$ (*bottom,* slower inactivation). The membrane potentials of the model heart (mHN$_c$) interneuron (unvaried) and the living heart (HN$_v$) interneuron (varied) and calcium conductance $g_{CaS,HNv}$ of the living heart interneuron are shown. Burst duration increased in the HN$_v$ interneuron with increasing η but was relatively constant in the mHN$_c$ interneuron. *B*: increasing I_{CaS} inactivation time constant (increasing η) in the HN$_v$ interneuron caused an increase in the period of the half-center oscillator (*top*), an increase of HN$_v$ interneuron's burst duration (*middle*) but not of the mHN$_c$ interneuron's burst duration, and little change in the final spike frequencies (f_{Final}) of either the mHN$_c$ or HN$_v$ interneuron (*bottom*). *, significant differences ($P < 0.05$) between measured values and values corresponding to $\eta = 1$. I_{SynS} and I_{CaS} in the living interneuron were blocked using Ca^{2+}-free Mn^{2+} saline. These currents were reinstated using dynamic clamp by artificial I_{SynS}, and artificial I_{CaS} with varied inactivation, both calculated in the real-time system.

Results for varying the inactivation time constant of I_{CaS} in the living neuron of a hybrid half-center oscillator were similar to those obtained when varying it in the model neuron of a hybrid half-center oscillator or of a model half-center oscillator (preceding text). In the example illustrated in Fig. 6*A*, decreasing I_{CaS} inactivation time constant (η) in living neuron of the hybrid half-center oscillator decreased its burst duration and the period of the oscillations (Fig. 6*A*, $\eta = 0.5$), while increasing I_{CaS} inactivation time constant had the opposite effects (Fig. 6*A*, $\eta = 4$). These manipulations had little effect on the burst duration of the model neuron or on the final frequency of either the model or living neuron. Figure 6*B* shows averaged data across preparations ($n = 6$). The period and the burst duration of the living neuron increased monotonically with η (Fig. 6*B*, *top* and *middle*; supplementary Table 2), and these effects were statistically significant [ANOVA $F(4,23) = 17.58$; $P = 9.78 \times 10^{-7}$ and $F(4,23) = 18.56$; $P = 6.17 \times 10^{-7}$, respectively]. The effect of varying η on f_{Final} (Fig. 6*B*, *bottom*) was significant [ANOVA $F(4,23) = 9.57$; $P = 1.04 \times 10^{-7}$] due to the notable decrease of f_{Final} for short I_{CaS} inactivation time constants ($\eta < 1$; Bonferonni *t*-test; $P = 1.09 \times 10^{-4}$ for $\eta = 0.25$ and $P = 4.07 \times 10^{-4}$ for $\eta = 0.5$); for long time constants ($\eta = 1, 2, 4$), f_{Final} was constant (Fig. 6*B*, bottom). As expected, the period was the same for both model and living heart interneurons. The burst duration and f_{Final} of the model neuron remained relatively constant as η was varied and there were no statistically significant effects of this variation [ANOVA $F(4,23) = 0.77$; $P = 0.56$, and $F(4,23) = 0.08$; $P = 0.99$, respectively].

In these experiments as in the previous model and hybrid system experiments, the decay time constant of g_{CaS} varied linearly with η (Fig. 4*C*, *left*), and there was a correlation between the decay time constants of g_{CaS} and of spike frequency in a burst (Fig. 4*C*, *right;* $r^2 = 0.70$; $n = 23$, $P = 7.2 \times 10^{-7}$). The fitting protocols used to assess these time constants are illustrated in Fig. 2 for data from these experiments. Figure 4 shows that for the three different types of experiments the two assessed times constants are well correlated, but in each case g_{CaS} decays faster than spike frequency. In the unvaried model heart neuron, there was no significant correlation between these time constants ($r^2 = 0.09$; $n = 28$, $P = 0.13$).

Spike frequency decay during the burst in heart interneurons recorded extracellularly in unmanipulated ganglia

Is the decay time constant of spike frequency, estimated in our hybrid system experiments where the time constant of I_{CaS} activation was varied in the living neuron (Fig. 2) similar to those in living half-center oscillators in unmanipulated leech ganglia? To answer this question, both heart interneurons in a ganglion were recorded extracellularly in the normal saline while the cells fired in alternating bursts. Exponential fits to spike frequencies decay in bursts from extracellularly recorded interneurons gave time constants in the range of 3.4–7.2 s (5.7 ± 1.6 s; $n = 6$, data not shown). These values are comparable to those observed in hybrid system experiments where the inactivation constant of I_{CaS} was varied in the living neuron; exponential fits of spike frequencies decay gave time constants in the range was 3.6 – 5.0 s (4.4 ± 0.3 s; $n = 6$) for canonical $\tau_{h,CaS}$ (i.e., $\eta = 1$).

Variation of I_{CaS} inactivation time constant in isolated living heart interneurons induced to burst autonomously with injected I_{CaS}

Our hybrid system experiments show that I_{CaS} inactivation time constant determines burst duration in heart interneurons in hybrid half-center oscillators. Do similar changes in the I_{CaS} inactivation time constant have similar effects on isolated living heart interneurons or is the presence of the opposing cell necessary for this effect? To address this question, we needed first to be able to reestablish intrinsic bursting activity in living heart interneurons synaptically isolated and with calcium currents blocked in Ca^{2+}-free Mn^{2+} saline by injecting I_{CaS} with dynamic clamp (Cymbalyuk et al. 2002b) (Fig. 1*E*, Table 1). Injecting of I_{CaS} with a maximal conductance of $\bar{g}_{CaS} = 3.2$ nS, as in the canonical model (Hill et al. 2001), never produced bursting. It was necessary to increase $\bar{g}_{CaS}$ and often, in addition, to hyperpolarize the cell with the constant injected current, I_{inject} (Fig. 1*E*). The following pairs of $\bar{g}_{CaS}$ (nS) and I_{inject} (nA) values were used in different preparations: (20, −0.4), (20, −0.1), (25, −0.15), (25, 0.02), (35, −0.3) ($n = 6$) and all produced regular bursting (for criterion see METHODS). The low-threshold slowly inactivating calcium current, I_{CaS}, therefore can support endogenous bursting in the living heart interneuron.

After endogenous bursting was initiated, we varied I_{CaS} inactivation time constant as described in the hybrid system experiments in the preceding text ($\eta = 1, 2, 4$). Despite the diversity of values of $\bar{g}_{CaS}$ and I_{inject} used for initiating bursting, the bursting in all ($n = 6$) preparations was quite consistent. Spiking usually ended before the end of burst plateaus in these experiments (Fig. 7*A*) thus necessitating a change in our measure of burst duration (see METHODS). In the example illustrated in Fig. 7*A*, $\eta = 1$, the period was 5.25 ± 0.52 s and burst duration was 2.34 ± 0.49 s. When the inactivation time constant of I_{CaS} was increased (Fig. 7*A*, $\eta = 2$ and $\eta = 4$), burst duration and period both increased. Figure 7*B* shows averaged data across preparations ($n = 6$); both period (Fig. 7*B*, *top*) and burst duration (Fig. 7*B*, *middle*) increased with increasing η and both these effects were significant [ANOVA $F(2,11) = 25.84$; $P = 7 \times 10^{-5,}$ and ANOVA $F(2,11) = 20.44$; $P = 2 \times 10^{-4}$ respectively; Fig. 7*B*; supplementary Table 3]. We measured f_{Final} for these "bursts" and found no variation with η [ANOVA $F(2,46) = 0.07$; $P = 0.93$]. We then compared these measures of $_{Final}$ with those from the experiments of Figs. 5*B* and 6*B* where η was varied in living neurons for $\eta = 1, 2, 4$. We found that f_{Final} was different among the three experiments [ANOVA $F(2,46) = 14.85$; $P = 0.000015$]. Post hoc testing with Dunnet's test revealed that for each value of η, f_{Final} was smaller for autonomous bursting than for hybrid system bursting with the single exception of hybrid system bursting in Ca^{2+}-free Mn^{2+} saline for $\eta = 2$ (Fig. 7*B*, *bottom*). This result indicates that during autonomous bursting the heart interneuron reaches a lower f_{Final} than during bursting in a hybrid half-center oscillator. We also estimated interburst intervals to check whether the variation I_{CaS} inactivation time constant affected interburst intervals in the absence of reciprocal inhibition (data not shown) and found no significant effect (ANOVA $F(2,11) = 1.92$; $P = 0.19$).

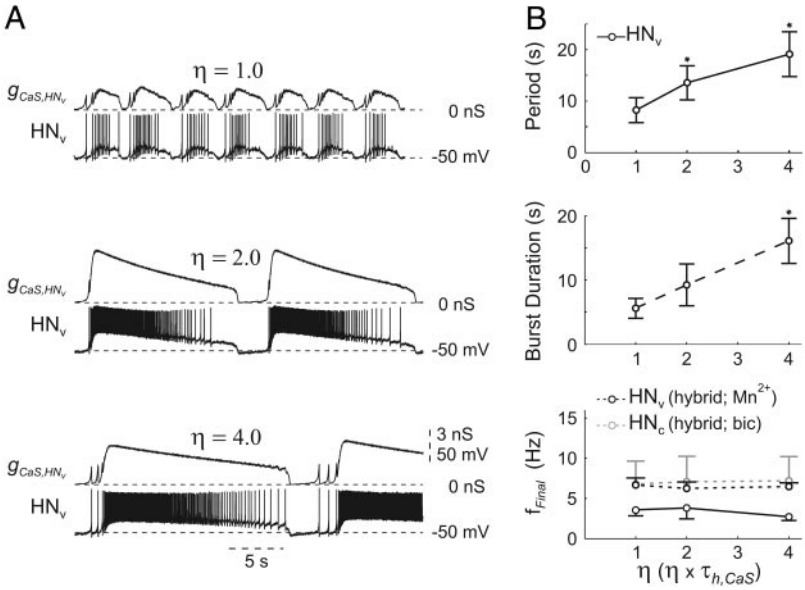

FIG. 7. Restoration of autonomous bursting in a synaptically isolated living heart interneuron, with the artificial I_{CaS}. *A*: typical behavior of a living heart (HN$_v$) interneuron for 3 different scaling factors of I_{CaS} inactivation time constant: η = 1 (*top,* faster inactivation), η = 2, (*middle,* inactivation as in the canonical model), and η = 4 (*bottom;* slower inactivation). The membrane potential of the living heart (HN$_v$) interneuron (varied) and calcium conductance $g_{CaS,HNv}$ of the living interneuron are shown. Burst duration increased in the HN$_v$ interneuron with increasing η but was relatively constant in the HN$_v$ interneuron. *B*: increasing I_{CaS} inactivation time constant (increasing η) in the HN$_v$ interneuron caused an increase in its period (*top*), an increase in its burst duration (*middle*), and no significant changes in its f_{Final} (*bottom*). Dunnet's test showed that the latter was significantly less than f_{Final} in hybrid system experiments (cf. Figs. 5*B* and 6*B*) in all but one pair-wise comparison [η = 1, 2, 4: P = 0.03, 0.049, 0.01 (Mn^{2+} - Ca^{2+}-free Mn^{2+} saline); P = 0.03, 0.055 (>0.05), 0.004 (bic - bicuculline saline)]. *, significant differences ($P < 0.05$) between measured values and values corresponding to η = 1. I_{SynS} and I_{CaS} in the living interneuron were blocked using Ca^{2+}-free Mn^{2+} saline. I_{CaS} was reinstated using dynamic clamp by artificial I_{CaS} with varied inactivation, calculated in the real-time system.

DISCUSSION

Here, we explored the intrinsic mechanisms by which burst duration in heart interneurons is controlled using a hybrid system approach that focused on the slowly inactivating low-voltage-activated (LVA) calcium current, I_{CaS}. We showed that the time constant of I_{CaS} inactivation determines the rate of spike frequency decline during a burst. During half-center alternating bursting activity, spike frequency in a burst declines to a final spike frequency, f_{Final}, that represents a critical level of effective inhibition from which by the opposite neuron can escape (Sorensen et al. 2004). Varying the I_{CaS} inactivation constant in a living or model interneuron, synaptically connected with an opposite living or model interneuron, did not affect final spike frequencies of either interneuron (Figs. 3, 5, and 6). The time constant of I_{CaS} inactivation and the time constant of spike frequency decay were in all cases strongly correlated (Figs. 2 and 4). This mechanism did not depend on the synaptic interaction with the opposite interneuron, it also held when the interneuron in which we varied I_{CaS} inactivation time constant was synaptically isolated (Fig. 7). We suggest that as in the hybrid system studied here that the inactivation of I_{CaS} is critically important for setting burst duration and thus period in the half-center oscillators that pace the leech heartbeat CPG.

Control of burst duration by decay of the excited state

Our results support the notion that burst duration in heart interneurons is determined by the decay of an excited state by slow inactivation of an inward current, I_{CaS}. A similar mechanism for control burst duration by decay of an inward current has been described in gastric mill pattern generator of crab stomatogastric nervous system (Coleman and Nusbaum 1994; Manor et al. 1999; Nadim et al. 1998). Here a mutually inhibitory pair of neurons, the lateral gastric neuron (LG) and interneuron 1 (Int1), are critical for generating the gastric mill rhythm. The LG receives a slow, modulatory, excitatory drive from a descending modulatory neuron MCN1 that activates an inward current. The LG locally, presynaptically inhibits that drive thus forming a negative feedback loop. The duration of the LG burst appears to be governed by the decay of the excitatory modulatory state once this presynaptic inhibition terminates modulatory action. Based on this hypothesis, modeling studies (Manor et al. 1999; Nadim et al. 1998) have shown that the de-activation time constant of the modulatory inward current determines the burst duration of LG. The burst duration of the opposite neuron, Int1, was not affected.

As in leech heart interneurons, LVA calcium currents (T-type calcium currents) promote and regulate neuronal bursting in many vertebrate systems (Huguenard 1996; Perez-Reyes 2003) including thalamocortical neurons (Fuentealba and Steriade 2005), inferior olivary neurons (Llinas and Yarom 1981), hippocampal pyramidal neurons (Fraser and MacVicar 1991), and cerebellar Purkinje neurons (Isope and Murphy 2005). The decay of LVA calcium current and associated Ca^{2+}-dependent nonselective cation current (I_{CAN}), appear to be crucial for various slow rhythms in thalamocortical neurons (Crunelli et al. 2005).

Restoration of autonomous bursting in heart interneurons with increased I_{CaS} introduced with dynamic clamp

Heart interneurons, pharmacologically isolated with bicuculline and recorded intracellularly with sharp microelectrodes fire tonically, i.e., they do not burst endogenously (Schmidt and Calabrese 1992). Because extracellularly recorded heart interneurons so isolated do burst endogenously (Cymbalyuk et al. 2002b), albeit at times intermittently, the failure to burst during sharp microelectrode recordings had been hypothesized to result from introduced nonspecific leak. Modeling studies support this hypothesis and show a narrow range of leak parameters that can support endogenous bursting (Cymbalyuk et al. 2002b). The same modeling studies indicate that the range of leak parameters capable of supporting bursting is enhanced with increased I_{CaS} (increased $\bar{g}_{CaS}$). By introducing large amounts of I_{CaS} into heart interneurons, isolated and with calcium current blocked in Ca^{2+}-free Mn^{2+} saline, we restored autonomous bursting during sharp microelectrode recording, although this often required small steady hyperpolarizing current in addition. This finding not only corroborates existing

hypotheses of how endogenous bursting arises in heart interneurons but provides a tool for future hybrid system studies. The hybrid half-center oscillators formed in the current study consisted of living neurons no longer able to express endogenous bursting and model neurons expressly tuned so they did not. We will now be able to explore the significance of endogenous bursting in hybrid-half center oscillators.

Interaction of I_{CaS}, I_h, and synaptic inhibition in the control of burst duration and period in a heart interneuron half-center oscillator

In the leech heartbeat CPG, mutually inhibitory pairs of heart interneurons form half-center oscillators that are the smallest circuit elements of the network. In the normal function of this elemental half-center oscillator, bursting is symmetric, with each neuron having a duty-cycle near 50% and the period thus being approximately twice the burst duration of either neuron (Hill et al. 2001). In this study, we showed that I_{CaS} inactivation time constant is an intrinsic regulator of burst duration in model and hybrid half-center oscillator, affecting only the burst duration of the specified interneuron and not of its opposite interneuron. When I_{CaS} inactivation time constant is varied unilaterally, symmetry in duty cycle is broken, and although period changes nearly linearly in step, it changes only in response to the nearly linear changes in the burst duration of the varied neuron. Symmetric changes in I_{CaS} inactivation time constant of course result in symmetric changes in burst duration and period twice the burst duration of either neuron. Given that inactivation time constants are not commonly observed to be modulated, can similar regulation of burst duration and period be expected with variation of $\bar{g}_{CaS}$, which can be expected to be modulated (Harris-Warrick 2002)? Previous modeling indicates that burst duration and period do vary smoothly with $\bar{g}_{CaS}$ albeit over a somewhat limited range (Hill et al. 2001). Altering $\bar{g}_{CaS}$, however, profoundly alters burst structure, dramatically increasing spike frequency and inhibition of the opposite neuron. Given that these same heart interneurons are important premotor elements of the CPG, modulating $\bar{g}_{CaS}$ will confound period changes with changes in the strength of premotor output.

How then can we expect period to be modulated in a heart interneuron half-center oscillator? Previous modeling (Hill et al. 2001) and the hybrid system analysis of Sorensen et al. (2004) indicates that I_h represents a potential control point. Variation in $\bar{g}_h$ leads to a smooth variation in period over a very broad range. I_h regulates, not burst duration, but interburst interval as might be expected by a current activated during the inhibited phase of the burst cycle. I_h promotes escape from inhibition of the opposite interneuron at a level of inhibition set by $\bar{g}_h$. This critical level of inhibition is that produced by the spike frequency at the end of the opposite interneuron's burst, f_{Final}. Asymmetric variation of $\bar{g}_h$ shows that increases/decreases in $\bar{g}_h$ act intrinsically to regulate interburst interval and thus indirectly through synaptic inhibition to decrease/increase the burst duration of the opposite interneuron, through escape at a higher/lower f_{Final}. Moreover, changes in $\bar{g}_h$ have only very modest effects on burst spike frequency structure. Thus modulation of $\bar{g}_h$ can achieve period control without confounding effects on premotor output. In this regard, we note that the neuropeptide myomodulin, which strongly accelerates period in heart interneurons, does so, at least in part, by increasing $\bar{g}_h$ but had no effect on either $\bar{g}_{CaS}$ or I_{CaS} inactivation time constant (Tobin and Calabrese 2005).

How then might variation of I_{CaS} inactivation time constant be harnessed for control of period and burst duration in heart interneurons? The I_{CaS} inactivation time constant can be thought of as setting a baseline period of a half-center oscillator that then can easily be modulated by modulating $\bar{g}_h$. This baseline limit is seen in the bursting of synaptically isolated heart interneurons recorded extracellularly (Cymbalyuk et al. 2002b) or in the restored autonomous bursting observed here (Fig. 7). With no inhibition to terminate I_{CaS}-mediated plateau depolarizations, inactivation directly terminates the plateau, and at canonical levels of $\bar{g}_{CaS}$, the burst cycle is dominated by the burst phase (Fig. 7) (Cymbalyuk et al. 2002b). Seen in this light, I_{CaS} inactivation time constant sets the dynamic range over which modulation of $\bar{g}_h$ can regulate the period of a heart interneuron half-center oscillator.

The level of $\bar{g}_h$ sets f_{Final} and thus the period of a half-center oscillator at a given $\bar{g}_{CaS}$, but I_{CaS} inactivation time constant sets how long it will take for a burst to evolve to f_{Find}. Alterations of I_{CaS} inactivation time constant do not have a large effect on the average frequency in a burst although they do alter burst frequency structure, owing to the gradual nature of spike frequency decline in a burst. Thus I_{CaS} inactivation time constant could serve a potential target for homeostatic control mechanisms that operate over a long time scale. For example, CPG period is much shorter in isolated nerve cords from juvenile leeches than from adults (Wenning et al. 2004). One potential mechanism could be alteration calcium-dependent inactivation of calcium currents potentially by changing buffer concentration/composition (Berridge et al. 2003). Calcium-dependent inactivation is a well-known phenomenon for high-voltage-activated calcium channels, particularly L-type channels (Budde et al. 2002; Findlay 2004) but is not known for T-type channels that are associated with LVA calcium currents (Huguenard 1998). However, Lu et al. (1997) provide data suggesting that the inactivation of LVA Ca currents in the leech heart interneuron is calcium-dependent. Regardless of the existence of mechanisms for modification, I_{Ca} inactivation time constant certainly acts in an important way to determine period in a heart interneuron half-center oscillator.

The joint control of bursting by I_{CaS} and I_h is not unique to leech heart interneurons. In particular, these currents both play an important role in thalamocortical relay neurons (Destexhe and Sejnowski 2003; McCormick and Huguenard 1992) by regulating waxing-and-waning "spindle" oscillations characteristic for a slow-wave sleep. Moreover, these currents operate in conjunction with strong synaptic inhibition as in heart interneurons (Fuentealba and Steriade 2005; Sohal et al. 2006). Together, this study and the study of Sorensen et al. (2004) provide an example of and clarify the interplay of the intrinsic cellular and extrinsic network regulation of burst duration and period in a half-center oscillator.

GRANTS

This work was supported by National Institute of Neurological Disorders and Stroke Grant NS-043098. The work of A. V. Olypher was partially supported by a Research Fellowship from Institut National de la Santé et de la Recherche Medicale.

REFERENCES

Angstadt JD and Calabrese RL. Calcium currents and graded synaptic transmission between heart interneurons of the leech. *J Neurosci* 11: 746–759, 1991.

Berridge MJ, Bootman MD, and Roderick HL. Calcium signalling: dynamics, homeostasis and remodelling. *Nat Rev Mol Cell Biol* 4: 517–529, 2003.

Budde T, Meuth S, and Pape HC. Calcium-dependent inactivation of neuronal calcium channels. *Nat Rev Neurosci* 3: 873–883, 2002.

Calabrese RL. Oscillation in motor pattern-generating networks. *Curr Opin Neurobiol* 5: 816–823, 1995.

Coleman MJ and Nusbaum MP. Functional consequences of compartmentalization of synaptic input. *J Neurosci* 14: 6544–6552, 1994.

Crunelli V, Toth TI, Cope DW, Blethyn K, and Hughes SW. The "window" T-type calcium current in brain dynamics of different behavioral states. *J Physiol* 562: 121–129 (Epub 2004 Oct 2021), 2005.

Cymbalyuk G, Sorensen M, Simoni MF, DeWeerth SP, and Calabrese RL. Software tools for hybrid system analysis. *Soc Neurosci Abstr* 28: 67.69, 2002a.

Cymbalyuk GS, Gaudry Q, Masino MA, and Calabrese RL. Bursting in leech heart interneurons: cell-autonomous and network-based mechanisms. *J Neurosci* 22: 10580–10592, 2002b.

Debay D, Wolfart J, Le Franc Y, Le Masson G, and Bal T. Exploring spike transfer through the thalamus using hybrid artificial-biological neuronal networks. *J Physiol* 98: 540–558, 2004.

Derjean D, Bertrand S, Le Masson G, Landry M, Morisset V, and Nagy F. Dynamic balance of metabotropic inputs causes dorsal horn neurons to switch functional states. *Nat Neurosci* 6: 274–281, 2003.

Destexhe A and Sejnowski TJ. Interactions between membrane conductances underlying thalamocortical slow-wave oscillations. *Physiol Rev* 83: 1401–1453, 2003.

Findlay I. Physiological modulation of inactivation in L-type Ca^{2+} channels: one switch. *J Physiol* 554: 275–283, 2004.

Fraser DD and MacVicar BA. Low-threshold transient calcium current in rat hippocampal lacunosum-moleculare interneurons: kinetics and modulation by neurotransmitters. *J Neurosci* 11: 2812–2820, 1991.

Fuentealba P and Steriade M. The reticular nucleus revisited: intrinsic and network properties of a thalamic pacemaker. *Prog Neurobiol* 75: 125–141, 2005.

Goaillard JM and Marder E. Dynamic clamp analyses of cardiac, endocrine, and neural function. *Physiology* 21: 197–207, 2006.

Harris-Warrick RM. Voltage-sensitive ion channels in rhythmic motor systems. *Curr Opin Neurobiol* 12: 646–651, 2002.

Hill AA, Lu J, Masino MA, Olsen OH, and Calabrese RL. A model of a segmental oscillator in the leech heartbeat neuronal network. *J Comput Neurosci* 10: 281–302, 2001.

Huguenard JR. Low-threshold calcium currents in central nervous system neurons. *Annu Rev Physiol* 58: 329–348, 1996.

Huguenard JR. Low-voltage-activated (T-type) calcium-channel genes identified. *Trends Neurosci* 21: 451–452, 1998.

Isope P and Murphy TH. Low threshold calcium currents in rat cerebellar Purkinje cell dendritic spines are mediated by T-type calcium channels. *J Physiol* 562: 257–269 (Epub 2004 Oct 2028), 2005.

Ivanov AI and Calabrese RL. Intracellular Ca^{2+} dynamics during spontaneous and evoked activity of leech heart interneurons: low-threshold Ca currents and graded synaptic transmission. *J Neurosci* 20: 4930–4943, 2000.

Ivanov AI and Calabrese RL. Modulation of spike-mediated synaptic transmission by presynaptic background Ca^{2+} in leech heart interneurons. *J Neurosci* 23: 1206–1218, 2003.

Kiehn O, Kjaerulff O, Tresch MC, and Harris-Warrick RM. Contributions of intrinsic motor neuron properties to the production of rhythmic motor output in the mammalian spinal cord. *Brain Res Bull* 53: 649–659, 2000.

Krahe R and Gabbiani F. Burst firing in sensory systems. *Nat Rev Neurosci* 5: 13–23, 2004.

Le Masson G, Renaud-Le Masson S, Debay D, and Bal T. Feedback inhibition controls spike transfer in hybrid thalamic circuits. *Nature* 417: 854–858, 2002.

Lisman JE. Bursts as a unit of neural information: making unreliable synapses reliable. *Trends Neurosci* 20: 38–43, 1997.

Llinas R and Yarom Y. Properties and distribution of ionic conductances generating electroresponsiveness of mammalian inferior olivary neurones in vitro. *J Physiol* 315: 569–584, 1981.

Lu J, Dalton JFt, Stokes DR, and Calabrese RL. Functional role of Ca^{2+} currents in graded and spike-mediated synaptic transmission between leech heart interneurons. *J Neurophysiol* 77: 1779–1794, 1997.

Manor Y and Nadim F. Frequency regulation demonstrated by coupling a model and a biological neuron. 38–40: 269, 2001.

Manor Y, Nadim F, Epstein S, Ritt J, Marder E, and Kopell N. Network oscillations generated by balancing graded asymmetric reciprocal inhibition in passive neurons. *J Neurosci* 19: 2765–2779, 1999.

Marder E. Plateaus in time. *Curr Biol* 1: 326–327, 1991.

Marder E and Calabrese RL. Principles of rhythmic motor pattern generation. *Physiol Rev* 76: 687–717, 1996.

Masino MA and Calabrese RL. Phase relationships between segmentally organized oscillators in the leech heartbeat pattern generating network. *J Neurophysiol* 87: 1572–1585, 2002.

McCormick DA and Huguenard JR. A model of the electrophysiological properties of thalamocortical relay neurons. *J Neurophysiol* 68: 1384–1400, 1992.

Nadim F, Manor Y, Nusbaum MP, and Marder E. Frequency regulation of a slow rhythm by a fast periodic input. *J Neurosci* 18: 5053–5067, 1998.

Olsen OH and Calabrese RL. Activation of intrinsic and synaptic currents in leech heart interneurons by realistic waveforms. *J Neurosci* 16: 4958–4970, 1996.

Perez-Reyes E. Molecular physiology of low-voltage-activated t-type calcium channels. *Physiol Rev* 83: 117–161, 2003.

Pike FG, Meredith RM, Olding AW, and Paulsen O. Rapid report: postsynaptic bursting is essential for "Hebbian" induction of associative long-term potentiation at excitatory synapses in rat hippocampus. *J Physiol* 518: 571–576, 1999.

Prinz AA, Abbott LF, and Marder E. The dynamic clamp comes of age. *Trends Neurosci* 27: 218–224, 2004.

Robinson HP and Kawai N. Injection of digitally synthesized synaptic conductance transients to measure the integrative properties of neurons. *J Neurosci Methods* 49: 157–165, 1993.

Schmidt J and Calabrese RL. Evidence that acetylcholine is an inhibitory transmitter of heart interneurons in the leech. *J Exp Biol* 171: 329–347, 1992.

Sharp AA, O'Neil MB, Abbott LF, and Marder E. Dynamic clamp: computer-generated conductances in real neurons. *J Neurophysiol* 69: 992–995, 1993.

Sohal VS, Pangratz-Fuehrer S, Rudolph U, and Huguenard JR. Intrinsic and synaptic dynamics interact to generate emergent patterns of rhythmic bursting in thalamocortical neurons. *J Neurosci* 26: 4247–4255, 2006.

Sorensen M, DeWeerth S, Cymbalyuk G, and Calabrese RL. Using a hybrid neural system to reveal regulation of neuronal network activity by an intrinsic current. *J Neurosci* 24: 5427–5438, 2004.

Szucs A, Varona P, Volkovskii AR, Abarbanel HD, Rabinovich MI, and Selverston AI. Interacting biological and electronic neurons generate realistic oscillatory rhythms. *Neuroreport* 11: 563–569, 2000.

Tobin A-E and Calabrese RL. Myomodulin increases I_h and inhibits the Na/K pump to modulate bursting in leech heart interneurons. *J Neurophysiol*: 00340.02005, 2005.

Wenning A, Hill AA, and Calabrese RL. Heartbeat control in leeches. II. Fictive motor pattern. *J Neurophysiol* 91: 397–409, 2004.

Willms AR, Baro DJ, Harris-Warrick RM, and Guckenheimer J. An improved parameter estimation method for Hodgkin-Huxley models. *J Comput Neurosci* 6: 145–168, 1999.